Instantaneous Receiver Operating Characteristic (ROC) Performance of Multi-Gain-Stage APD Photoreceivers

George M. Williams, David A. Ramirez, Majeed M. Hayat, and Andrew S. Huntington

***Abstract*—We describe the use of analytical and numerical models of a multi-gain-stage single-carrier multiplication (SCM) avalanche photodiode (APD) to generate time-resolved receiver operating-characteristic (ROC) curves. First, pseudo-DC analytic models of discrete multi-stage APDs are used to generate the statistical properties of the SCM APD necessary for ROC analysis. Next, numerical models are used to develop the joint probability density function (PDF) of the SCM APD gain and avalanche buildup time as a function of the device structure, material properties and local electric fields. The instantaneous (time-resolved) carrier count distributions resulting from photon- and dark-initiated impact ionization chains are used to calculate the mean and variance of the currents induced in the circuits of the photoreceiver over the integration times of the detection event. Last, autocorrelation functions are generated to allow the parameters of the signal, the noise and the signal embedded in noise—which are necessary for ROC hypothesis testing—to be calculated for the instances of the impulse response. It is shown that time-resolved ROC analysis of an APD photoreceiver, which includes the instantaneous properties of photon- and dark-initiated avalanche events, allows for better optimization of photoreceiver performance than does non-time-resolved ROC analysis.**

***Index Terms*—APD, avalanche photodiode, excess noise, false alarm rate, impulse response, photoreceiver, probability of detection, receiver sensitivity, shot noise**

I. Introduction

A. Properties of Avalanche Photodiode Receivers

AVALANCHE photodiodes (APDs) are widely used photodetectors in optical receivers deployed in laser rangefinders, laser radar imagers, optical communications systems and other applications. An advantage of APDs is their ability to provide high internal optoelectronic gain. Amplifier circuit noise is the dominant noise source in high bandwidth photoreceivers assembled from unity-gain photodiodes; when APDs are used, the internal current gain of the APD improves the receiver's signal-to-noise ratio (SNR) by boosting the photocurrent signal beyond the downstream amplifier circuit noise. However, APD avalanche gain, M, also multiplies its shot noise, and the shot noise increases faster than the photocurrent signal by a factor of $\sqrt{F}$, where the excess noise factor, F, is greater than or equal to one. Moreover, the rate of primary dark current generation inside an APD increases with reverse bias, so shot noise, prior to multiplication, also increases with M. Thus, although amplifier circuit noise dominates at low values of M, the excess noise factor and dark current characteristics of the APD determine an optimal gain for every APD/amplifier combination. Beyond this point, increased M degrades photoreceiver SNR. The excess noise factor results from the stochastic nature of avalanche multiplication and is usually analyzed and measured in the low frequency limit. However, since most pulse detection circuits trigger off of photocurrent transients rather than the total integrated photocharge, there are circumstances in which analysis of the instantaneous photocurrent and dark current pulse height statistics are required [1]–[5].

To allow high avalanche gain without the deleterious effects of excess noise, various approaches have been used. These approaches include the use of thin multiplication regions [6] and the use of impact-ionization engineered multiplication regions [7], [8]; both approaches exploit dead-space effects to reduce excess noise. Unfortunately, APDs designed to exploit dead-space effects are generally capable of only low avalanche multiplication levels [9], [10].

To achieve high gain and low excess noise, superlattice, graded-gap and staircase APDs [11], [12], [13], [14] have been proposed. These APD designs generally use multiple, discrete heterostructured gain stages to promote preferential ionization of one carrier over the other, so that significant enhancement of the effective hole–electron ionization ratio, k, is made possible. In APDs of this type, high gain and very low avalanche noise is achieved if: 1) A large number of gain stages exist; 2) The impact ionization events occur only in discrete locations of the multiplication layer; 3) Mostly one carrier impact ionizes, i.e., either electrons or holes, thereby reducing or, preferably, eliminating the excess noise associated with ionization feedback from the other carrier type; and 4) For the preferred carrier type, the probability of ionizing in each gain stage approaches unity.

Manuscript received May 10, 2013; revised July 2, 2013; accepted July 27, 2013. Date of publication September 5, 2013; date of current version October 21, 2013. The review of this paper was arranged by Editor A. G. U. Perera.

G. M. Williams and A. S. Huntington are with Voxtel Inc., Beaverton, OR 97006 USA (e-mail: georgew@voxtel-inc.com; andrewh@voxtel-inc.com).

D. A. Ramirez and M. M. Hayat are with the Center for High Technology Materials, University of New Mexico, Albuquerque, NM 87106 USA (e-mail: dramirez@skinfrared.com; hayat@chtm.unm.edu).

Color versions of one or more of the figures in this paper are available online at http://ieeexplore.ieee.org.

Digital Object Identifier 10.1109/JEDS.2013.2280892

B. Single-Carrier Multiplication APDs

We developed a discrete multi-gain-stage single-carrier multiplication (SCM) APD that is realized in the InAlGaAs material system. The back-illuminated SCM APDs: have 1.5-μm-thick $In_{0.53}Ga_{0.47}As$ absorbers; are responsive from 950 nm to 1700 nm; and are limited on the short wavelength side by absorption in the InP substrate. What sets this device apart from standard InGaAs APDs, is that rather than a monolithic semiconductor multiplication region, the SCM APD is made of a cascade of 200-nm thick *p-i-p-i-n-i* InAlAs/InAlGaAs heterostructured gain stages, each designed to spatially modulate the electric field and material ionization thresholds to favor local electron ionization over hole ionization [15].

In operation of the SCM APD, photons arrive at the detector aperture and generate Poisson-distributed electron-hole pairs; the absorber is located on the anode side of the multiplier, so only primary photoelectrons are injected into the multiplier.

Upon injection into the multiplier, the primary photoelectrons impact-ionize with probability P in each of the J multiplying stages they transit on the path to the cathode. Each impact ionization generates a secondary electron-hole pair; on the path back to the anode, secondary holes impact-ionize with probability U per stage encountered.

Since electrons and holes are counter-propagating and either carrier type can impact-ionize in any stage transited, impact-ionization chains can circulate multiple times through the multiplier. Each potential impact-ionization event is subject to chance, so the more branching possibilities an impact-ionization chain has, the greater the statistical variation of the gain. Preventing one carrier type from impact-ionizing greatly constrains the variety of impact-ionization chains that are possible, minimizing the noise of the gain process.

In an ideal SCM APD, holes do not impact ionize; assuming negligible contributions from hole-ionization feedback, $U \rightarrow 0$. In the ideal case, each primary photoelectron contributes an average gain of approximately $M = (1 + P)^J$ during the time, T, it transits the J gain stages of the multiplication region [13], [15], [16]. For example, assuming $P = 0.7$, a 10-stage InGaAs/InAlAs SCM APD with no hole ionization feedback will achieve a gain of $M \approx 202$.

However, while the low excess noise associated with single-carrier ionization is desirable, in many practical high-gain SCM APD designs, there is a probability that holes will ionize in each gain stage, i.e., $U > 0$. For example, a hole-ionization rate, β, to electron-ionization rate, α, ratio of $k = 0.02$ has been demonstrated in SCM APDs operating at gains exceeding $M = 1024$ [15]. When hole-ionization feedback occurs, a higher mean DC gain is achieved—as a result of a two-carrier multiplication process—than occurs with just one ionizing carrier. As a result, the avalanche impulse response is longer in duration than the time required for the electrons and holes created during $T = 1$ transit times to clear the junction. Also, because of two-carrier ionization, there is greater uncertainty in the magnitude of the signal over the instances of the impulse response [16], [17]. These characteristics govern the performance of an SCM APD-enabled photoreceiver.

Fig. 1 plots the accumulated gain and the excess noise of the partial gain as a function of avalanche buildup time, expressed as multiples of the average carrier junction transit time [16]. The plot was generated using numerical models of the SCM APD.

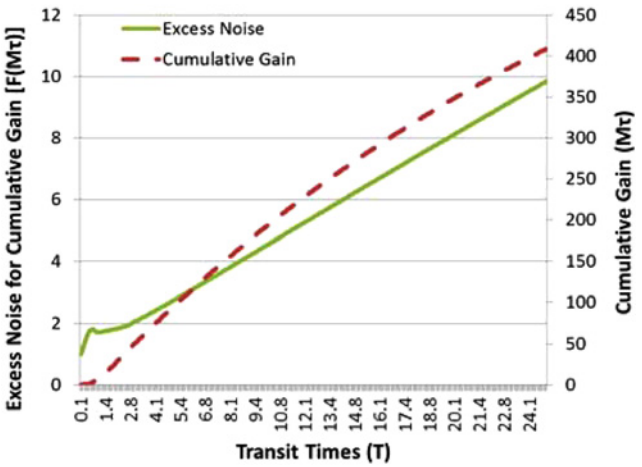

Fig. 1. Cumulative instantaneous excess noise factor of an SCM APD biased for DC gain of $M_{DC} = 937$, plotted as a function of the average transit time of the multiplication region by a carrier.

Factors determining which signal a photoreceiver's decision circuits monitor are: distributions of photocurrent pulse height, dark current pulse height, and timing; and the distribution of amplifier noise. The influence of avalanche gain variability on photoreceiver performance can be quantified by studying the resultant receiver operating characteristic (ROC). The influence of variability in the time and magnitude of the avalanche gain can be quantified by studying the ROC performance over the times of the impulse response.

C. Receiver Operating Characteristic

ROC analysis offers a comprehensive way to describe APD photoreceiver performance [18], [19]. For any given detector, a ROC curve plots the probability of detection, $P_{DE,}$ as a function of the probability of false alarm, P_{FA}. For two detectors operating with the same P_{FA}, if the P_{DE} of one detector is greater than the other, it can be concluded that the greater P_{DE} detector is more effective than the other.

ROC analysis casts the detection problem as a binary decision problem, i.e., a binary hypothesis testing problem. Although there are only two possible mutually exclusive hypotheses at any moment for the conclusion that there is a signal present or not, there are two possible outcomes for each answer; each conclusion is either correct or incorrect. The four possible outcomes, which are shown in Fig. 2, are:

1) *True Positive (TP):* The optical signal is present and is detected by the photoreceiver. This is also termed the detection probability, P_{DE}:

$$P_{DE} = \int_{thresh}^{\infty} p_{s+n}(n)\, dn, \tag{1}$$

where p_{s+n} is the normalized distribution of the sum of the signal and noise, and *thresh* is the detection threshold of the decision circuit. The distribution of the signal plus noise can be analyzed by convolving APD pulse height distribution (including both signal photocurrent and dark current) with the

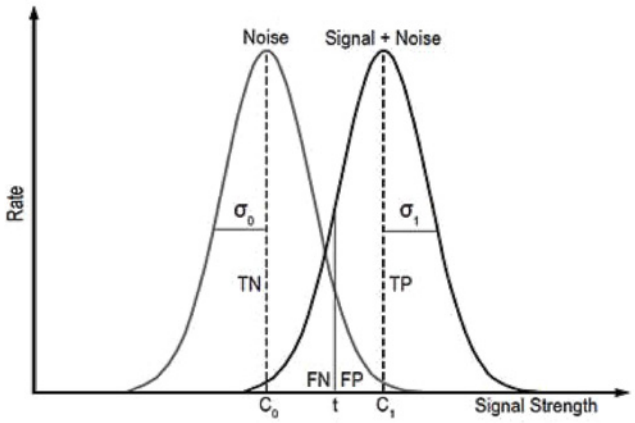

Fig. 2. Generic internal response probability of occurrence curves for noise-alone and for signal-plus-noise trials.

amplifier circuit noise distribution, applying the rule that the distribution of the sum of two independent random variables is given by the convolution of their distributions.

2) *False Negative (FN):* The optical signal is present but is not detected by the photoreceiver; $P_{FN} = 1 - P_{DE}$.

3) *False Positive (FP):* The optical signal is not present but the photoreceiver registers a spurious detection. This is also termed the probability of false alarm, P_{FA}:

$$P_{FA} = \int_{thresh}^{\infty} p_n(n)\, dn, \tag{2}$$

where p_n is the normalized distribution of the noise. As with p_{s+n}, p_n can be analyzed by convolving APD dark current pulse height distribution with amplifier circuit noise distribution.

4) *True Negative (TN):* The optical signal is not present and the photoreceiver does not register detection; $P_{TN} = 1 - P_{FA}$.

II. Analytical Models of SCM APD Low-frequency (Pseudo-DC) Signal and Noise Characteristics

Using the probability density function (PDF) and low order statistical models of the APD, (1) and (2) can be used to perform APD photoreceiver ROC analysis.

A. Multiplied Signal in an SCM APD

The multiplied signal across the terminals of an APD implemented in a photoreceiver, I_s, in response to a signal with optical power, P_{opt}, is modeled as:

$$I_s = M \left(\eta q / h\upsilon\right) P_{opt}, \tag{3}$$

where M is APD gain, η is APD unit gain quantum efficiency, q is charge of an electron, h is Planck's constant, and v is frequency of the photon.

For an SCM APD with quantity J gain stages, the avalanche gain of the SCM APD has been shown to be approximated as [12]:

$$M_J = \frac{P - U}{P\,(1+U)\left(\dfrac{1+U}{1+P}\right)^J - U\,(1+P)} = \frac{1-k}{(1+k\,P)\left(\dfrac{1+k\,P}{1+P}\right)^J - k\,(1+P)} \tag{4}$$

B. Noise Sources of the SCM APD Photoreceiver

Generally, noise sources in an APD photoreceiver include: 1) amplifier circuit noise; 2) shot noise of the photoelectrons, often described by Poisson statistics [20]; 3) uncertainty in mean avalanche gain, characterized by the excess noise factor; and 4) shot noise and excess noise of the multiplied dark current.

1) *Amplifier Circuit Noise:* The common sources of electrical noise, including Johnson (or thermal) noise, either obey or approximate a Gaussian distribution because of the central limit theorem. Similar to the (discrete) Poisson distribution, the (continuous) Gaussian distribution fits the description of a "well-behaved" distribution, having maximum probability density at the mean value of random variable, $< n >$, falling off symmetrically and rapidly to either side of $< n >$.

2) *Poisson Shot Noise:* The absorption of light and the diode leakage processes, such as thermal generation and trap-assisted tunneling, respectively generate primary photocurrent (I_{aphoto}) and primary dark current (I_{adark}). Photon arrival, primary dark current generation, and the transit of charge carriers across barriers (as in a diode junction) are all statistically independent events; when these processes are stationary (characterized by a fixed average rate of occurrence) they obey Poisson statistics. For a given sample time, the number of electrons transported across the junction, a, fluctuates around its mean value, $< a >$, with a variance equal to its mean. The shot noise of these primary currents is defined as the standard deviation of a, equal to the square root of the mean value; in current terms, spectral intensity of shot noise is given by Schottky's theorem: $S_I = 2qI_a$, where q is elementary charge, and I_a is primary current. Although the (discrete) Poisson distribution should be used when the carrier count a is small, in the limit of large sample sizes, the approximation of a (continuous) Gaussian distribution with variance equal to its mean can be used for convenience.

3) *Excess Multiplication Noise:* In an APD, the primary carriers generated by a given Poisson process, a, are multiplied by impact-ionization, yielding a total, n, that is related to the primary carrier count by a gain factor, m. If the gain process were deterministic and m were a constant m_0, the variance of the total would be $var(n) = m_0^2 var(a) = m_0^2 < a >$. However, in most APDs, gain is a random variable, and:

$$\mathrm{var}(n) = \langle m \rangle^2 \frac{\langle m^2 \rangle}{\langle m \rangle^2} \langle a \rangle = M^2\, F\, \langle a \rangle \tag{5}$$

where $M = < m >$ is the average gain, and the ratio of the average square gain to the square of the average gain, F, is called the excess noise factor because it represents the proportional increase of the carrier count variance relative to the case

of deterministic gain; in current terms, spectral intensity of multiplied shot noise is given by Schottky's theorem, enhanced by the same factor: $S_I = 2qM^2FI_a$. A general expression for F was derived by van Vliet for the case in which the primary current into the multiplier consists solely of electrons [12]:

$$F_J(M_J) = 1 + \frac{(M_J - 1)(1-k)}{M_J(2+P+k\,P)} \times \left[-P + 2\left(\frac{1-k\,P^2}{1+k\,P}\right)\left(M_J\,k\frac{1+P}{1-k} + \frac{1}{1+P}\right)\right] \quad (6)$$

where $k = U/P$. When values of M_J and P consistent with (4) are used, (6) approximates the excess noise factor of a J-stage SCM APD. Van Vliet's expression for F reduces to the commonly used form of McIntyre [23], $F_J = M_J[1 - (1 - k)(M_J - 1)^2/M_J^2]$, in the limit $J \to \infty$, which applies to most APDs with homogenous multiplying junctions.

Many analyses of P_{DE} and P_{FA} assume that the output distribution of multiplied photocurrent and dark current in an APD are Gaussian-distributed, such that the shape of the output distribution is well characterized by the variance given in (5). The central limit theorem ensures that this is a good approximation in the limit of a large number of primary carriers; however, since the output distribution of most APDs for single-carrier input has a strong positive skew, the approximation is poor in the limit of photon counting.

Other complications include the distinction between low-frequency gain versus instantaneous photocurrent in an APD, and the dependence of the gain distribution upon where primary carriers are injected into the multiplier. Common pulse detection systems use comparators that are triggered when APD instantaneous photocurrent exceeds an adjustable detection threshold. If the avalanche gain process lasts longer than the APD junction transit time, the photocurrent peak height distribution will not be the same as the APD low-frequency gain distribution, since some of the primary and secondary photocarriers generated in response to an optical signal will exit the junction before all the secondaries have been generated. Moreover, trap-assisted tunneling in the high-field regions of the multiplier is the dominant source of primary dark current in an SCM APD, so generation of primary dark current carriers is distributed throughout the multiplier, whereas all primary photoelectrons are generated in a separate absorption layer and are injected into the multiplier at the anode-facing end. The mean gain of the photocurrent is greater than that of the dark current because the path length through the multiplier is longer, and gain distributions are different because of the greater variation in primary dark current injection location and associated path length through the multiplier; injection of pure electron-only photocurrent from the absorber versus mixed electron-and hole injection from primary dark current also differentiates the respective gain distributions [21].

4) *Excess Noise of Multiplied Dark Events:* In the SCM APD, the dark carrier generation rate, Φ, is often dominated by carrier tunneling from the high field regions of the distributed gain stages. As a result, count distributions of multiplied dark carriers have a different mean avalanche gain and variance than multiplied photoelectrons [22].

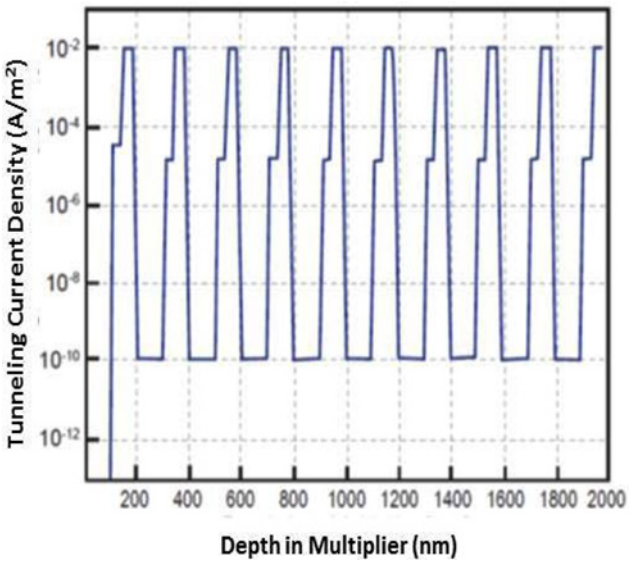

Fig. 3. Modeled dark current generation rate as a function of location in the SCM APDs multiplication layer ($x = 0$ is the location of photoelectron injection [22].

Fig. 3 shows a spatially-resolved model of the unmultiplied dark carrier density generation in the SCM APD multiplication layer, calculated from [5], assuming a 100-micrometer diameter SCM APD operating at room temperature. The areas of highest dark carrier density in Fig. 3 correspond to the highest electric field region of each of the SCM APD gain stages. Dark carriers generated in each of the individual gain stages induce in the external circuits a current signal that is a function of their spatial origin. As the dark carriers are generated randomly in the gain stages, the mean amplitude of the signal induced in the circuits by the dark carriers is lower in magnitude and higher in variance than the current induced by the photoelectrons that originate in the absorber and traverse all of the gain stages [22].

O'Reilly and Fyath address the issue of multiplied shot noise on dark current generated throughout the multiplier of an APD by finding an effective excess noise factor that gives the correct variance when applied to the gain-normalized terminal dark current. That is, they treat the dark current as though primary dark current were generated in the absorber, subject to the same gain as the photocurrent [14]. However, approximating the dark current pulse height distribution as a Gaussian distribution with a variance determined by O'Reilly's effective F does not work well for single primary carrier injection. The discrepancy is illustrated in Fig. 4 (top), which compares two analytic pulse height distributions to two numerical distributions generated by a one-million-trial Monte Carlo calculation, for a 10-stage SCM APD operated at an average photocurrent gain of $M_{10} = 404$ and characterized by $k = 0.004$ (the average gain of the dark current is found to be just $M = 75$ due to the shorter path length through the multiplier). The curve labeled "Averaged McIntyre" is a better fit than the Gaussian curve; the averaged McIntyre curve treats the dark

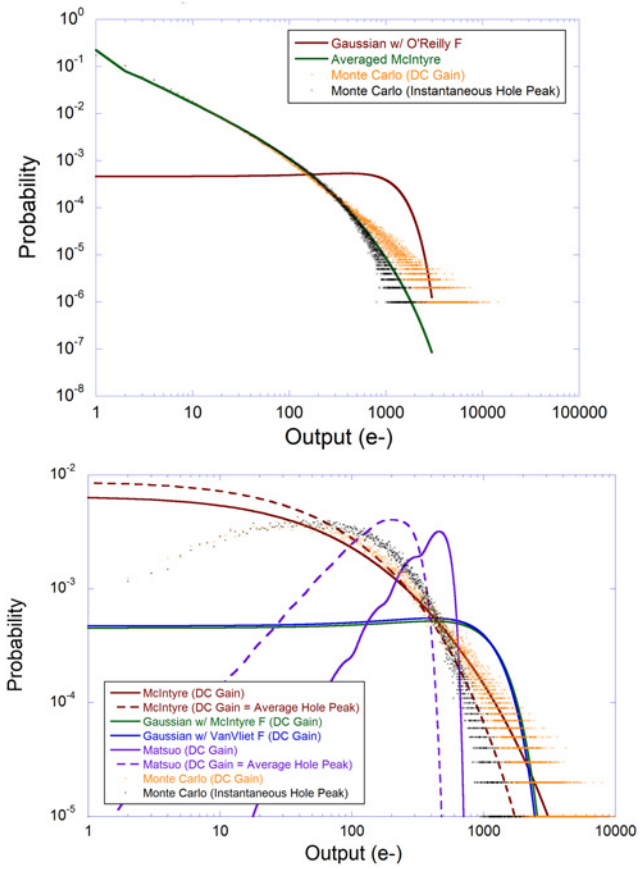

Fig. 4. Comparison of analytic and Monte Carlo gain distributions for dark current (top) and photocurrent (bottom) of a 10-stage SCM APD operated at an average photocurrent gain of $M = 404$, and an effective impact ionization coefficient ratio of $k = 0.004$.

current as though a primary dark carrier pair generated in stage j of J total stages has the pulse height statistics of a single electron injected into the first stage of a $J - j$ stage multiplier. This approximation neglects the possibility of holes impact-ionizing in stages preceding j and neglects the contribution of hole feedback between stages to the total gain. The average of McIntyre distributions written for each value of j between 0 and $J - 1$ is used to reflect uniform probability of dark current generation amongst all J stages, and because primary carriers are generated in the middle of a given stage, they don't pick up enough energy to impact-ionize before exiting their stage of origin:

$$p(n) = \frac{1}{J}\sum_{j=0}^{J-1} p_{McIntyre}\left(1, n, m_{stage}^{j}, k\right) \tag{7}$$

where m_{stage} is the gain-per-stage in the approximation of electron-only avalanche:

$$m_{stage} = \sqrt[J]{M_J} \tag{8}$$

and $p_{McIntyre}(a,n,M,k)$ is the McIntyre distribution for an output of n carriers resulting from injection of a primary electrons into a multiplier characterized by average gain M and effective impact ionization coefficient ratio k [23]:

$$\begin{aligned} &p_{McIntyre}(a, n, M, k)\big|_{M=1} = \delta_{a\,n}; \\ &p_{McIntyre}(a, n, M, k)\big|_{M>1} = \frac{a \times \Gamma\left(\frac{n}{1-k}+1\right)}{n\,(n-a)\,! \times \Gamma\left(\frac{kn}{1-k}+a+1\right)} \\ &\times \left[\frac{1+k\,(M-1)}{M}\right]^{a+\frac{kn}{1-k}} \times \left[\frac{(1-k)\,(M-1)}{M}\right]^{n-a} \end{aligned} \tag{9}$$

in which Γ denotes the Euler gamma function. The two Monte Carlo distributions plotted in Fig. 4 (top) correspond to the distribution of gain in the low-frequency limit (i.e., the distribution of the total output carrier count, integrated over the complete impulse response) and that of the maximum number of holes simultaneously in the APD junction, which is a surrogate for the peak height of the dark current pulse. The hole count is used for the impulse response statistics because holes travel a much longer path from their point of generation to the anode than do the electrons to the cathode, and so are the dominant contribution to SCM APD current.

Fig. 4 (bottom) makes similar comparisons for several different analytic models of the pulse height distribution of the photocurrent. Whereas primary dark current generation was distributed uniformly across the ten high-field AlGaInAs impact-ionization layers of the SCM APD multiplier in the Monte Carlo simulation plotted in Fig. 4 (top), in Fig. 4 (bottom), primary photocarrier injection occurs in the absorber, distributed according to the absorption envelope for 1550-nm light; 100000 trials were run to generate the photocurrent statistics. The two curves labeled "McIntyre (DC Gain)" and "McIntyre (DC Gain = Average Hole Peak)" correspond to (9) for $M = 404$ and $M = 211$, respectively. Although (9) applies only to the low-frequency gain of the APD, it was adapted to analyze the height distribution of the peak of the impulse response by using an effective gain of $M = 211$, which is the average across all Monte Carlo trials of the maximum hole population in the junction (effectively, the average impulse response peak height). The two analytic distributions labeled as "Gaussian" apply (6) to compute the variance of a Gaussian distribution centered on an average gain of $M = 404$; "McIntyre F" uses the form of (6) that applies in the limit $J \to \infty$. Finally, the curves labeled "Matsuo" show the counting distribution of a hypothetical staircase APD with strictly electron-only multiplication, published by Matsuo et al. [23]

Fig. 4 illustrates that low order statistical measures, such as the excess noise, fail to take into consideration the carrier count distributions, as they do not provide a complete statistical description of the multiplied photon and dark carriers. They are thus insufficient for accurate ROC analysis of APD receivers.

Furthermore, in an APD, the variance of the gain process can vary over the span of the avalanche buildup time as different groups of carriers propagate through the multiplier. Due to the complex interplay between the buildup time and the gain, and to describe accurately the pulse detection process, one must appeal to the complete statistical analysis of the times of the APD impulse response. Thus, while pseudo-DC gain and excess noise measures are useful for describing APD photoreceivers operating under low frequency signal conditions, such as when the optical pulse is longer than the impulse response, they do not accurately describe a photoreceiver pulse

detection process under the most practical operating scenarios in which short optical pulses are used [13].

Lacking accurate closed form analytical models of the partial gain over the times of an APD impulse response, numerical models of the instantaneous excess noise of the cumulative partial gain are required.

III. Numerical Models of SCM APD Impulse Response

The P_{DE} and P_{FA} values required for APD photoreceiver ROC analysis necessitate a more complete statistical description of the current, such as those found in the carrier counting distributions. Indeed, P_{DE} and P_{FA} performance measures are especially dependent on the tails of the counting distributions, which are generally only weakly reflected in the excess noise factor.

Furthermore to model accurately the signals induced in the external circuits by multiplied photon and dark signals over integration times shorter than the optical pulse duration, the multiplied carrier count distributions must be known for each instance of the impulse response [16], [22]. In order to model statistically the integrated photocurrent over the integration times of the decision circuits, the autocorrelation function of the photo and dark signals is also necessary [24].

To describe the instantaneous gain and noise performance of the SCM APD, we developed an extension of the Dead Space Multiplication Theory (DSMT) [25], [26], which enabled us to determine the spatial and temporal distribution of the electron and hole impact ionization events.

The DSMT's recursive equations were modified to include carrier energy relaxation effects and, for the dark current, primary carrier injection throughout the multiplier, so that the PDFs of the electron and hole populations of the junction could be calculated as functions of time for both dark current and photocurrent [16]. The low-order statistics of the photocurrent and dark current were calculated from the carrier population statistics as a function of time by application of the Shockley-Ramo Theorem [27].

Fig. 5 shows the instantaneous mean and variance of photocurrent and dark current over $T = 25$ junction transit times, calculated by the DSMT for the 10-stage SCM APD described in detail in [15]. The calculation of dark current impulse response statistics assumes generation of primary dark current is distributed through the multiplier as shown in Fig. 3.; the photocurrent calculation assumes primary photoelectron injection at the edge of the multiplier

The models assumed the SCM APD included a 1.5-μm thick InGaAs absorption region and a 2-μm thick multiplication region formed by 10 200-nm thick heterostructured gain stages. Assuming, for the sake of simplicity, equal electron and hole carrier velocities of about 10^6 cm/s, which was estimated from the impulse response curves of [16], the transit time of a 10-stage InAlAs multiplication region can be estimated to be approximately 200 ps.

In a ROC curve, the true positive (TP) rate is plotted as a function of the false positive (FP) rate for different threshold settings. Each point on the ROC curve represents a TP/FP

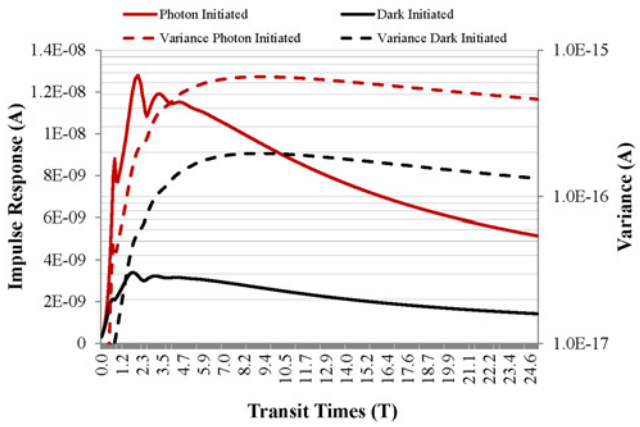

Fig. 5. Numerically modeled impulse response from photoelectrons ($x = 0$) and the mean of the dark carriers generated randomly in the gain stages of a 10-stage SCM APD.

(sensitivity/specificity) pair corresponding to a particular decision threshold. Our approach to including APD instantaneous properties in the photoreceiver ROC analysis using the time-resolved PDFs and statistical models of the SCM APD, was to solve the signal detection problem in which, based on an optimal threshold test at each time of the impulse response, it was decided whether a signal was present or not. For the instances of the impulse response, we constructed the carrier PDFs for both: 1) the case in which the signal was embedded in noise; and 2) the case in which only amplifier and dark noise were present. We used the MGFs to generate low-order statistical moments at each time of the impulse response, assuming that the probability densities are normally distributed with mean, μ, and variance, σ^2.

To generate the ROC curves, the null hypothesis was tested by calculating the partially integrated stochastic photocurrent due to dark carriers in the integration interval $\{0, T_b\}$. T_b was expressed at multiples of T transit times, and the dark carriers were assumed to be generated randomly throughout the high field regions of the device.

The pair of parameters generated for the case when only dark current noise was present, included the mean given by [17]:

$$\mu_0 = \varphi \int_0^{Tb} \int_0^{t} \left\langle \overline{I_p}(t-\xi) \right\rangle d\xi dt \tag{10}$$

where $\overline{I_p}(t)$ is the mean impulse response of the dark carriers (calculated from Fig. 3) and the variance is given by:

$$\sigma_0^2 = \varphi \int_0^{Tb} \int_0^{Tb} \int_0^{u \wedge v} \overline{R_{Ip}}(u-\xi, v-\xi) d\xi du dv \tag{11}$$

where $\overline{R_{Ip}}(t_1, t_2)$is the autocorrelation function of the dark carriers averaged over the multiplication region, as shown in Fig. 6.

The autocorrelation function calculated for the photon signal is shown in Fig. 7.

The alternative hypothesis was calculated, over the interval $\{0, T_b\}$ by integrating the photon-triggered signal pulse

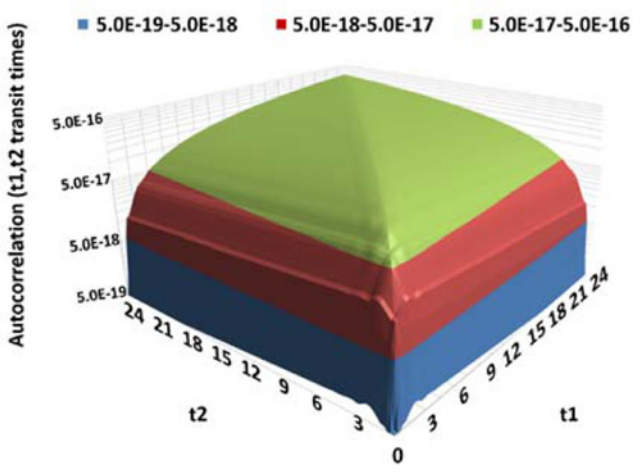

Fig. 6. Auto-correlation of SCM APD dark-generated events over 25 transit times.

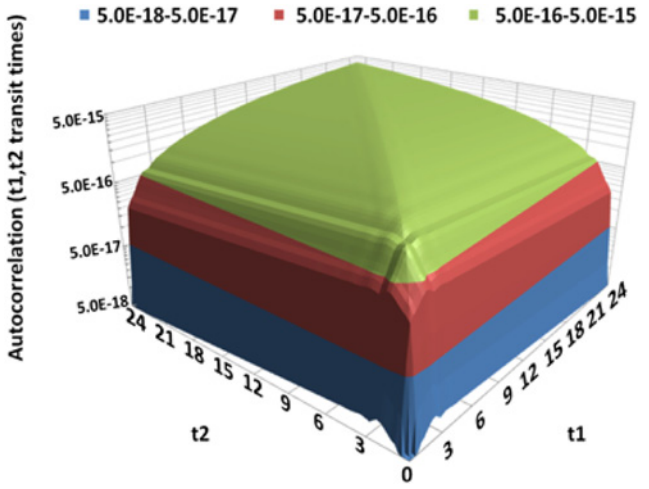

Fig. 7. Auto-correlation of SCM APD photon events over 25 transit times.

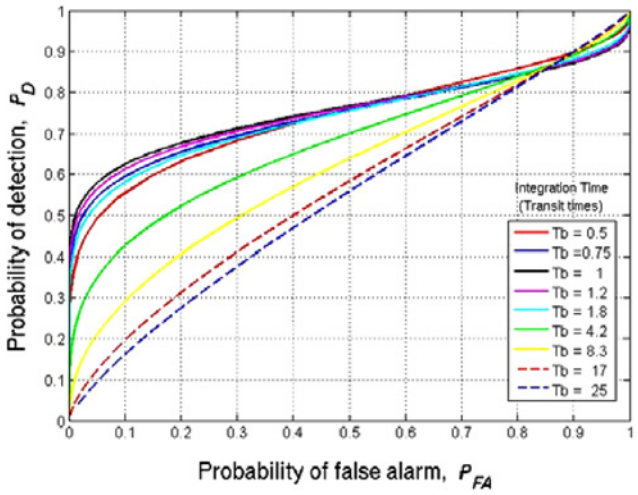

Fig. 8. ROC curve for a 10-stage SCM APD with the dark current generation rate shown in Fig. 3, without contributions from amplifier noise, i.e., APD only.

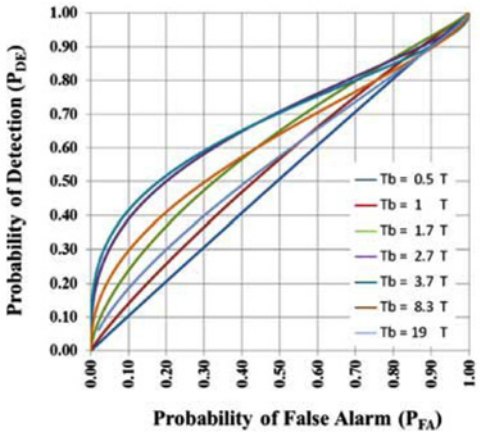

Fig. 9. ROC curves shown as a function of the integration time T_b. The curves were calculated including a 42 e- RMS amplifier and an InGaAs absorption layer.

embedded in the noise of the integrated dark current. The mean and the variance of the alternative hypothesis are given by:

$$\mu_1 = \mu_0 + \int_0^{Tb} \langle I_p(t) \rangle \, dt \tag{12}$$

and

$$\sigma_1^2 = \sigma_0^2 + \int_0^{Tb} \int_0^{Tb} R_{Ip}(u, v) du dv. \tag{13}$$

Using the parameters for each hypothesis, the ROC curve of Fig. 8 was expressed as a function of the number of integrated carrier transit times for a 10-stage SCM APD, assuming no electronic amplifier noise.

It can be seen by examination of Fig. 8 that assuming no noise contributions from amplifier circuit noise, the area under the ROC curves reaches a maximum at $T_b \approx 1$T transit times (approximately the peak of the impulse response shown in Fig. 5. For integration times longer than $T_b > 1$T transit times, P_{DE} decreases due to the deleterious effects of the cumulative excess noise of the partial gain of the photosignal and dark current contributions, which dominate the signals at longer integration times.

Fig. 9 shows ROC curves for the 10-stage SCM-APD photoreceiver, in which an amplifier with a Johnson noise source equivalent to 42 e- RMS, is included. For any P_{FA}, the P_{DE} of Fig. 9 is reduced from the ideal case of Fig. 8.

When including amplifier noise sources, the noise floor is greater and longer integration times are necessary. As a result the area under the ROC curve occurs later in the impulse response than is the case when only the APD is considered. Under these conditions, in Fig. 9 the area under the ROC curve is optimal for a signal integrated at approximately $T_b = 3.7$ transit times (approximately 740 ps).

Fig. 10 and Fig. 11 show the P_{FA} and P_{DE} components, respectively, of the ROC curve shown in Fig. 9. In these figures, each curve is expressed as a function of the threshold setting; for convenience, each curve is expressed in terms of gain for single-photon inputs. In these figures, it is clear that at approximately $T_b = 3.7$ transit times, the SCM APD partial gain is sufficient to overcome the 42 e- RMS amplifier

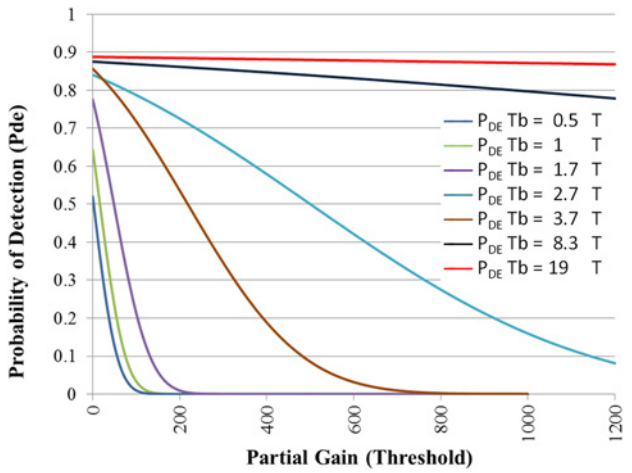

Fig. 10. Probability of false alarm as a function of the threshold including the equivalent of 42 e- RMSJohnson noise from the amplifier.

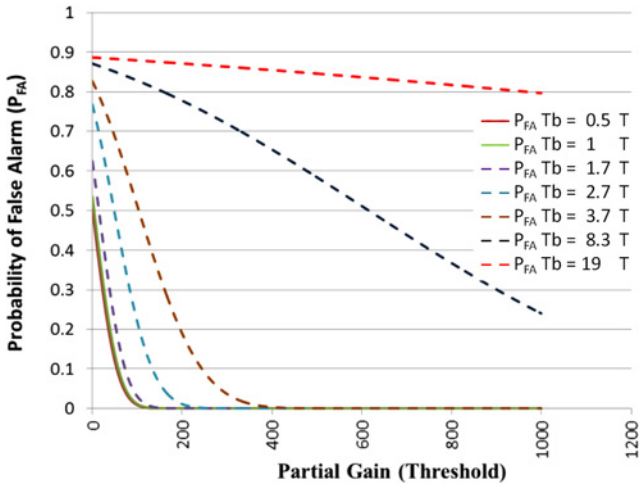

Fig. 11. Probability of detection as a function of the threshold including an amplifier Johnson noise contribution of 42 e- RMS.

noise. From Fig. 1, we can determine that at approximately 3.7 transit times, the partial gain is approximately $M\tau = 80$. At longer integration times, although P_{DE} increases at all threshold levels, at each setting P_{FA} also increases due to increase in accumulated multiplied photon- and dark-carrier excess noise.

IV. Summary

We have demonstrated the ability to use numerical models of the instantaneous properties of a multi-gain-stage SCM APD to predict the performance of an SCM APD threshold receiver over the instances of the APD photoreceiver's impulse response most relevant to pulse detection. It is shown that due to the bias-dependent instantaneous avalanche multiplication properties of an APD impulse response, in cases where the optical pulse is shorter than the impulse response function (non-instantaneous gain), the pseudo-DC avalanche gain properties most often used to characterize APD performance are inadequate for describing photoreceiver performance.

In most practical applications it is necessary to perform ROC analysis over the instances of the receiver's impulse current response. In the case of the SCM APD, modified DSMT models allow PDFs of the current signal induced in the circuit by photon-initiated and dark-initiated avalanche events to be calculated for the times of the impulse response, so that instantaneous statistical moments of avalanche events can be determined, allowing for the probabilities of detection and false alarm rate to be calculated as a function of integration time. The time-varying properties of the generated ROC curves illustrate the significance of using this approach to describe accurately the performance of APD photoreceivers.

While we have demonstrated this approach to photoreceiver ROC analysis for the single-photon response to a 10-stage SCM APD, this approach can similarly be used to model the response of a photoreceiver so as to describe multi-photon pulse signals and other dark carrier generation rates, such as those that might result from smaller diameter and cryogenically cooled APD receivers, including those not configured with SCM APDs.

References

[1] R. J. McIntyre, "Multiplication noise in uniform avalanche diodes," *IEEE Trans. Electron. Devices*, vol. 13, no. 1, pp. 164–168, Jan. 1966.
[2] P. Bhattacharya, *Semiconductor Optoelectronic Devices,* 2nd ed. Upper Saddle River, NJ, USA: Prentice Hall, 1997, p. 384.
[3] B. E. A. Saleh and M. C. Teich, *Fundamentals of Photonics*. New York, NY, USA: Wiley, 1991.
[4] M. C. Teich, K. Matsuo, and B. E. A. Saleh, "Excess noise factors for conventional and superlattice avalanche photodiodes and photomultiplier tubes," *IEEE J. Quantum Electron.*, vol. 22, no. 8, pp. 1184–1193, Aug. 1986.
[5] S. R. Forrest, "Performance of InGaAsP photodiodes with dark current limited by diffusion, generation recombination and tunneling," *IEEE J. Quantum Electron.*, vol. 17, no. 2, pp. 217–226, Feb. 1981.
[6] M. M. Hayat, O. Kwon, Y. Pan, P. Sotirelis, J. C. Campbell, B. E. A. Saleh, and M. C. Teich, "Gain-bandwidth characteristics of thin avalanche photodiodes," *IEEE Trans. Electron. Devices*, vol. 49, no. 5, pp. 770–781, May 2002.
[7] S. Wang, R. Sidhu, X. G. Zheng, X. Li, X. Sun, A. L. Holmes, Jr., and J. C. Campbell, "Low-noise avalanche photodiodes with graded impact-ionization-engineered multiplication region," *IEEE Photon. Technol. Lett*., vol. 13, no. 12, pp. 1346–1348, Dec. 2001.
[8] M. M. Hayat, O. H. Kwon, S Wang, J. C. Campbell, B. E. A. Saleh, and M. C. Teich "Boundary effects on multiplication noise in thin heterostructure avalanche photodiodes: Theory and experiment," *IEEE Trans. Electron. Devices*, vol. 49, no. 12, pp. 2114–2123, Dec. 2002.
[9] W. Sun, X. Zheng, L. Zhiwen, and J. C. Campbell, "Monte Carlo simulation of InAlAs/InAlGaAs tandem avalanche photodiodes," *IEEE J. Quantum Electron.*, vol. 48, no. 4, pp. 528–532, Apr. 2012.
[10] J. P. Gordon, R. E. Nahory, M. A. Pollack, and J. M. Worlock, "Low-noise multistage avalanche photodetector," *IEEE Electron. Lett.*, vol. 15, no. 17, pp. 518–519, Aug. 1979.
[11] F. Capasso and W.T. Tsang, "Superlattice, graded band gap, channeling and staircase avalanche photodiodes towards a solid-state photomultiplier," in *Proc. IRE Int. Electron. Devices Meeting,* vol. 28, 1982, pp. 334–337.
[12] K. M. van Vliet, A. Friedmann, and L. M. Rucker, "Theory of carrier multiplication and noise in avalanche devices—Part II: Two-carrier processes," *IEEE Trans. Electron. Devices*, vol. 26, no. 5, pp. 752–764, May 1979.
[13] K. Matsuo, K. B. Saleh, and M. Teich, "Excess noise factors for conventional and superlattice avalanche photodiodes and photomultiplier tubes," *IEEE J. Quantum Electron.*, vol. 22, no. 8, pp. 1184–1193, Aug. 1986.
[14] J. J. O'Reilly, and R. S. Fyath, "Analysis of the influence of dark current on the performance of optical receivers employing superlattice APDs," *IEE Proc. J Optoelectron. U.K.*, vol. 135, no. 2, pp. 109–118, Feb. 1988.

[15] G. M. Williams, M. Compton, D. A. Ramirez, M. Hayat, and A. S. Huntington, "Multi-gain-stage InGaAs avalanche photodiode with enhanced gain and reduced excess noise," *IEEE J. Electron. Devices Soc.*, vol. 1, no. 2, pp. 54–65, Feb. 2013.
[16] G. M. Williams, D. A Ramirez, M. M. Hayat, and A. S. Huntington, "Time resolved gain and excess noise properties of InGaAs/InAlAs avalanche photodiodes with cascaded discrete gain layer multiplication regions," *J. Appl. Phys.*, vol. 113, no. 9, p. 093705, Mar. 2013.
[17] P. Sun, M. M. Hayat, B. E. A. Saleh, and M. C. Teich, "Statistical correlation of gain and buildup time in APDs and its effects on receiver performance," *J. Lightw. Technol.*, vol. 24, no. 2, pp. 755–768, Feb. 2006.
[18] H. Poor, *An Introduction to Signal Detection and Estimation*. New York, NY, USA: Springer-Verlag, 1988, ch. 2.
[19] H. L. Van Trees, *Detection, Estimation and Modulation Theory, Part I*. New York, NY, USA: Wiley, 1968.
[20] D. G. Youmans, G. M. Williams, and A. S. Huntington, "Linear-mode avalanche photo-diode detectors with a quasi-deterministic gain component: Statistical model studies," in *Proc. SPIE Laser Radar Technol. Appl. XVI,* vol. 8037, Jun. 2011, p. 803716.
[21] R. J. McIntyre, "The distribution of gains in uniformly multiplying avalanche photodiodes: Theory," *IEEE Trans. Electron. Devices*, vol. 19, no. 6, pp. 703–713, Jun. 1972.
[22] G. M. Williams, D. A. Ramirez, M. M. Hayat, and A. S. Huntington, "Discrimination of photon- and dark-initiated signals in multiple gain stage apd photoreceivers," *IEEE J. Electron. Devices Soc.*, vol. 1, no. 4, pp. 99–110, Apr. 2013.
[23] K. Matsuo, M. C. Teich, and B. E. A. Saleh, "Noise properties and time response of the staircase avalanche photodiode," *J. Lightw. Technol.*, vol. LT-3, no. 6, pp. 1223–1231, 1985.
[24] M. M. Hayat and B. E. A. Saleh, "Statistical properties of the impulse response function of double-carrier multiplication avalanche photodiodes including the effect of dead space," *J. Lightw. Technol.,* vol. 10, no. 10, pp. 1415–1425, Oct. 1992.
[25] M. M. Hayat, B. E. A. Saleh, and M. C. Teich, "Effect of dead space on gain and noise of double-carrier multiplication avalanche photodiodes," *IEEE Trans. Electron. Devices*, vol. 39, no. 3, pp. 546–552, Mar. 1992.
[26] M. A. Saleh, M. M. Hayat, B. E. A. Saleh, and M. C. Teich, "Dead-space-based theory correctly predicts excess noise factor for thin GaAs and AlGaAs avalanche photodiodes," *IEEE Trans. Electron. Devices*, vol. 47, no. 3, pp. 625–633, Mar. 2000.
[27] S. Ramo, "Current induced in electron motion," in *Proc. IRE*, vol. 27, Sep. 1939, pp. 584–585.

George M. Williams is the President of (Voxtel, Inc.) Beaverton, OR, USA, and oversees Voxtel's Research and Development and commercial product sales. He also contributes technically in the engineering of X-ray, UV, visible, NIR, infrared, night vision, and multi-spectral EO systems. He has been involved in researching, designing, and manufacturing image sensors, imaging systems, and image processing algorithms for over 25 years. His specific technical expertise includes active and passive electro-optical system design and modeling, as well as silicon CCD and CMOS, InGaAs, image intensified detector, and HgCdTe detector design and manufacturing. He also takes an active lead in nanocrystal-based photovoltaics, thermoelectric coolers, and upconverting and downconverting nanocrystal film device development. Previously, as Executive VP and General Manager of PixelVision, Inc. and its sister company, SITe, Inc.,

Mr. Williams managed the teams that designed, manufactured, and delivered CCD technology to a variety of commercial and important government programs, including imagers for the Hubble Space Telescope SITS and Advanced Camera, SOHO, as well as other important NASA (Space Shuttle, Chandra, etc.) and DoD missions. While at ITT Night Vision, he developed considerable experience in image-intensified night vision goggles (NVGs) and infrared detector design and development, and led the commercialization of the night vision technology in the NightMariner and NightEnforcer product lines. Mr. Williams holds a DoDTop Secret security clearance.

David A. Ramirez is a Research Scientist at SKINfrared LLC. Albuquerque, NM USA. He received the B.S. and M.Sc. degrees in electrical engineering from the University of Concepción, Chile, USA in 2002 and 2005, respectively. In 2012, he graduated with a Ph.D. in Electrical Engineering from the University of New Mexico. His research interests include the design and fabrication of infrared photodetectors, numerical modeling of semiconductor devices, and scientific computing with Python. In January 2012, He was awarded a Post-Doctoral fellowship by the New Mexico Cancer Nanoscience and Microsystems Training Center (CNTC) to carry out cancer research. Since then, he has been collaborating with the multidisciplinary group at SKINfrared LLC that is focused on skin cancer research. At SKINfrared LLC, Dr. Ramirez is involved with the development of an Advanced Longwave Infrared-imaging and Analysis System (ALIAS), fabrication of next generation infrared devices, and the numerical modeling of semiconductor devices.

Majeed M. Hayat received the Bachelor of Science (*summa cum laude*) in electrical engineering from the University of the Pacific, Stockton, CA, USA in 1985, and the M.S. and Ph.D. degrees in electrical and computer engineering from the University of Wisconsin-Madison, Wisconsin, USA in 1988 and 1992, respectively. He is currently a Professor of Electrical and Computer Engineering, Associate Director of the Center for High Technology Materials, and General Chair of the Optical Science and Engineering Program at the University of New Mexico. Dr. Hayat's research activities cover a broad range of topics including avalanche photodiodes, signal and image processing, algorithms for spectral and radar sensing and imaging, optical communication, networked computing, and modeling interdependent networks with applications to smart grids. Dr. Hayat was an Associate Editor of *Optics Express* from 2004 to 2009 and he is currently the Chair of the topical committee of Photodetctors, Sensors, Systems and Imaging within the IEEE Photonics Society. He was a recipient of the National Science Foundation Early Faculty Career Award (1998) and the Chief Scientist Award for Excellence (2006) from the National Consortium for MASINT Research of the Defense Intelligence Agency. Dr. Hayat has authored or co-authored over 82 peer-reviewed journal articles (H-Index = 27) and has six issued patents, three of which have been licensed. Dr. Hayat is a Fellow of SPIE and OSA.

Andrew S. Huntington manages Voxtel's Detector Development Group and is responsible for Voxtel's advanced development efforts relating to semiconductor devices, material growth, device modeling, and detector design and development efforts. He invented and patented Voxtel's advanced high-gain, low-excess-noise SCM-APD technologies, and has supported this important device's development through Monte Carlo modeling and experimental extraction of the material's properties. He has also managed the development of Voxtel's array process and APD-based commercial products. The detector projects Dr. Huntington has conducted include Geiger- and linear-mode SOICMOS and InGaAs-based APDs for the NIR;HgCdTe APDs for the SWIR, MWIR, and LWIR; and silicon-based linear APDs for visible and X-ray applications. He has a number of publications detailing this work. Prior to joining Voxtel, Dr. Huntington persued doctoral studies in materials at the University of California, Santa Barbara (L. Coldren Group), CA, USA where his dissertation work included development of low-noise and broad-area InGaAs/InAlAs APDs. That work was conducted in collaboration with Professor Joe Campbell of the University of Texas, Austin, who is widely recognized as a leader in the field. Conducting this work, Dr. Huntington developed his expertise in the production of APD wafers by molecular beam epitaxy, with particular emphasis on understanding the relationship between growth conditions, material quality, and device performance. Dr. Huntington holds a DoD Secret security clearance.